Phosphorescent Probes in Studies of Secondary Relaxation of Amorphous Polystyrene and Poly(*n*-alkyl methacrylate)s

M. Christoff and T. D. Z. Atvars*

Departamento de Físico-Química, Instituto de Química, Universidade Estadual de Campinas, Caixa Postal 6154, CEP 13083-970, Campinas, SP, Brazil

Received January 5, 1999; Revised Manuscript Received May 29, 1999

ABSTRACT: Phosphorescence from four aromatic ketones (xanthone, benzophenone, flavone, and 9-methoxyflavone) has been used to study secondary α-, *β*-, and *γ*-relaxation processes in polystyrene and poly(*n*-alkyl methacrylate)s (*n*-alkyl = methyl, ethyl, and butyl) in the temperature range 15−400 K. Plots of normalized phosphorescence intensity versus temperature and the respective Arrhenius curves showed changes of nonradiative deactivation efficiencies, which were attributed to polymer secondary relaxation processes. In addition to the phosphorescence emission, flavones in poly(*n*-alkyl methacrylate)s also exhibited fluorescence emission ascribed to the protonated moiety. The presence of these two emissions indicated a probe distribution sensing two different microenvironments: protic (fluorescent) and nonprotic (phosphorescent) sites. Protic sites reveal the existence of acidic residues copolymerized to the methacrylic polymer chains. Plots of fluorescence intensity versus temperature have been used to determine the polymer relaxation processes of these acidic domains always revealing a higher onset temperature compared to the phosphorescence emission. The influence of both the size and the shape of these probes has also been analyzed, demonstrating that small molecules (xanthone and benzophenone) are more sensitive to shorter segmental motions occurring at lower temperatures.

I. Introduction

Unlike the crystalline state, cooled amorphous polymers present a glassy structure characterized by a disordered solid structure. Around the glass transition temperature (T_g) large changes in the mechanical and transport properties have been observed. The mechanism of these changes is strongly dependent on the polymer matrix, on the type of property being measured, and on the temperature range. At temperatures below T_g, the diffusional motions and structural changes involving short segments and end groups become highly restricted, but relatively faster relaxation of the vibrational and librational degrees of freedom are possible.[1−3] Despite the normal Arrhenius-like temperature dependence of the several types of thermal-activated processes, slow motions of polymer chains (α-relaxation process) exhibit strong temperature dependence described by the Williams−Landel−Ferry (WLF) equation.[4] Moreover, at T_g the time scale for structural relaxation is within minutes and involves several types of main-chain dynamic processes. On the other hand, localized motions involving side groups or short segments persist in the glassy state and have been observed to follow an Arrhenius-like temperature dependence for the average correlation time.[3,5,6]

Recent studies of poly(*n*-alkyl methacrylate)s have focused on the nature of the motions involved with the secondary relaxation processes.[6−13] While the secondary relaxations are considered as the *β*-process, involving motions of side groups of the macromolecule, the α-relaxation process has been attributed to the main-chain rotation. Depending on the temperature and on the *n*-alkyl group size, α- and *β*-relaxation processes can be coupled. Indeed, results obtained with NMR techniques for poly(methyl methacrylate) (PMMA) revealed that the dynamics of both the ester moiety and the methyl side groups (*β*-relaxation) may be coupled with main-chain motions (α-relaxation process).[6,7,13] In addition, experiments using dielectric relaxation demonstrated different thermokinetic structures with greater complexity depending on the size of the side groups involved with *β*- and α-relaxation coupling in poly(*n*-alkyl methacrylate)s.[10] Although the coupling between α- and *β*-relaxation processes has been shown by several experimental techniques, the dependence of the relaxation processes on the size of the alkyl derivatives remained unclear.[9,13−16]

Polymer secondary relaxation mechanisms have been studied by several instrumental methods such as dielectric spectroscopy,[10] NMR,[6,9,17−19] positron annihilation spectroscopy,[12,20,21] luminescence spectroscopy, and other techniques.[7,11,13,22−28] Luminescence spectroscopy is very attractive for determining the onset temperatures for polymer relaxation processes due to the strong temperature dependence of photophysical properties of probe or label groups in the polymeric material. Several types of spectroscopic techniques can be used, including steady-state or time-resolved measurements, radiative or radiationless processes, and anisotropy measurements.[29,30] Moreover, it is possible to select intrinsically or extrinsically luminescent polymers, and in the case of nonluminescent polymers, we can choose a large number of available probes covering a wide variety of shapes, sizes, solubilities, and photophysical and photochemical properties.[5,23,24] Usually, the high sensitivity of techniques requires a reduced amount of the external probe, ensuring a small disturbance of the polymer matrix.[24]

Considering the Arrhenius-like temperature dependence of the local macromolecular motions below T_g, low-frequency measurements or long-term observations should be useful for a better discrimination of the temperature range related to the onset of each second-

* To whom all correspondence should be addressed. e-mail: tatvars@iqm.unicamp.br.

10.1021/ma990008x CCC: $18.00 © 1999 American Chemical Society
Published on Web 08/20/1999

Scheme 1

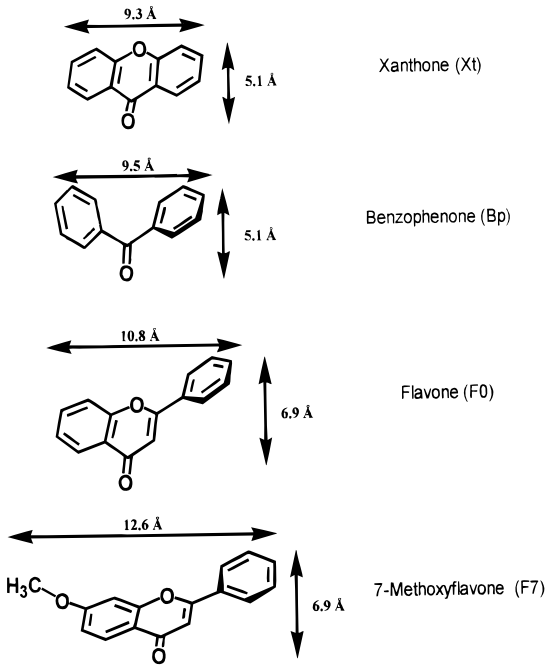

ary transition.[5,22] Indeed, the temperature dependence of the long-lived phosphorescent state has been useful to determine the onset of some lower temperature local motions of several polymers[5,22] while the short-lived fluorescent state has been more useful to follow higher temperature processes.[29−31] In a previous work we determined the onset temperatures for thermal relaxation processes of cross-linked poly(ethyl acrylate) networks measuring the temperature dependence of the fluorescence emission of anthracene dissolved or anthryl groups bonded to the network chains.[32] This work showed that the onset temperatures were almost the same independent of the fluorescent moiety and that the major differences were related to the bandwidth of the whole spectra. We have also shown that the temperature dependence was roughly of Arrhenius type for both probes.

The present work is an attempt to study the temperature dependence of the photophysical properties of four phosphorescent aromatic carbonyl derivatives dissolved in poly(*n*-alkyl methacrylate)s (methyl-, ethyl-, and *n*-butyl-) and polystyrene (as a nonpolar reference medium). The choice of the molecular probes (benzophenone, xanthone, flavone, 7-methoxyflavone) (Scheme 1) was based on the following criteria: (1) these probes have different molecular shapes and sizes; (2) their photophysical properties should be strongly related to both their structures and specific dye/polymer interaction; and (3) they exhibit high phosphorescence quantum yields ($\phi_{Ph} > 0.4$) with variable degree of mixing between n−π* and π−π* transitions of the low-lying excited triplet state.[33−37] Moreover, benzophenone has been chosen due to its well-known photochemical properties in several polymer media, and the temperature dependence of the triplet state decay profiles was ascribed to the hydrogen abstraction by the excited molecule, producing a ketyl radical.[38,39]

The low-lying triplet state of benzophenone (^{3}Bp*) exhibits a dominant n−π* character,[33] being shifted to higher energy (blue) as the medium polarity increases. On the other hand, the low-lying xanthone triplet state (^{3}Xt*) is strongly dependent on the media polarity promoting an inversion from n−π* to π−π* as the polarity decreases.[33] Moreover, the larger ^{3}Xt* dipole moment of the excited state compared to the electronic ground state may lead to a different exciplex structure and stability between the n−π* or π−π* probe and the energy acceptor group.[34,35] Flavone (F0) and 7-methoxyflavone (F7) are phosphorescent molecules in nonprotic media, but protonation of the carbonyl group promotes a simultaneous radiative deactivation by fluorescence emission.[35−37] Furthermore, the internal free rotation around σ-bonds external to the benzopyrone ring may contribute to a nonradiative deactivation pathway of the electronic excited state. Compared to flavone, the 7-methoxyflavone contains a methoxy group that is expected to introduce another type of physical hindrance to the accommodation of the molecule in the polymer matrix, requiring a larger free-volume site. While the benzophenone and xanthone average sizes are similar (v_w = 169.3 and 165.2 Å^3, respectively) their molecular shapes are different, changing from planar (Xt) to a twisted molecule (Bp). These molecular volumes were calculated using the atomic increment method.[40] On the other hand, flavones are larger ($v_{w\ (F0)}$ = 413 Å^3 and $v_{w(F7)}$ = 436.3 Å^3), with the free-rotating phenyl substituent introducing a volume element to the molecular shape. For comparison, the molecular volume of the alkyl groups are 48.3, 63.5, and 99.3 Å^3 for methyl acrylate, ethyl acrylate, and butyl acrylate groups, respectively.[40] In addition, we estimated by molecular modeling (MM_2) the most stable geometry of these molecular probes that resulted in the planar dimension showed in Scheme 1: xanthone < benzophenone < flavone ≈ 7-methoxyflavone. These probes with different shapes and sizes were chosen in an attempt to correlate the photophysical properties to the available free-volume produced by the alkyl side group of the polymer matrix.

II. Experimental Section

7-Methoxyflavone (F7) was obtained by methylation of the corresponding hydroxyflavone (Aldrich Chemical Co.) in the presence of an excess of diazomethane. F7 was recrystallized at least three times from cyclohexane. Benzophenone (Bp), xanthone (Xt), and flavone (F0) (Aldrich Chemical Co.) were recrystallized from ethanol at least two times before using. All of these molecules were kept in the dark until use.

The following polymers were used as received: polystyrene (PS) (EDN), poly(methyl methacrylate) (PMMA) (Aldrich cod. [9001-14-7]), poly(ethyl methacrylate) (PEMA) (Aldrich cod. [9003-42-3]), and poly(butyl methacrylate) (PBMA) (Aldrich cod. [9003-63-8]). Preliminary tests using these polymers revealed the presence of residual acid groups copolymerized in the polymer chain.[41] Exhaustive Soxhlet extraction using ethyl acetate and in sequence ethanol solvents were unable to remove these acidic residuals. Thus, the purification step was abandoned, and they were used as received.

Films of these polymers were physically characterized by several techniques: the glass transition temperatures were determined by differential scanning calorimetry, DSC (Du Pont, model v2.2A 990), calibrated with indium as a standard. Two scans were performed for every sample: the first scan heated the sample from room temperature to 150 °C, then the sample was quenched at −150 °C, and finally, it was heated again to 150 °C. The heating rate was 10 °C/min. The glass transition temperatures are listed in Table 1. The molecular weights and polydispersities were determined by GPC (Waters), with a IR 410 refractive index detector and using tetrahydrofuran as eluent at a temperature of 40 °C. Polystyrene was used as the standard.

Table 1. Glass Transition Temperatures (DSC) and Molecular Weights (by GPC) for the Polymer Films

	T_g (K)	$M_n \times 10^{-4}$ (g mol^{-1})	$M_w \times 10^{-5}$ (g mol^{-1})	polydispersity
PS	378	7.1	1.8	2.5
PMMA	368	9.2	2.4	2.6
PEMA	337	7.5	1.6	2.1
PBMA	298	4.7	1.1	2.3

Films of the polymers (PS, PMMA, PEMA, PBMA) were prepared by casting their dichloromethane (Aldrich Chemical Co.) solutions on silanized Petri dishes (to avoid adhesion).[42] Polymer films containing the luminescent probes were prepared by adding a certain volume of $(2-4) \times 10^{-3}$ mol L^{-1} stock dichloromethane solution containing both probe and polymer. A selected volume was defined for a desired probe/polymer composition ratio, established to give a detectable phosphorescence signal without probe aggregation in the matrix. The prepared films were dried at room temperature in air. Once formed, these films were kept for a couple of weeks in a desiccator under vacuum. One day before use, they were annealed at 60 °C in an oven for 8 h and kept in it until measurements were performed. Film thickness was ca. 300 μm. No solvent residuals were detected by gravimetric thermal analysis.

Luminescence measurements at various temperatures were performed as described elsewhere.[31,43,44] The samples were inserted into a cryosystem kept under vacuum throughout measurements.[44] The experimental temperature range was 15−405 K. Electronic absorption spectra of all probes, in solution or dissolved in polymer matrices, were recorded on a Hewlett-Packard 8452 spectrophotometer at room temperature. A 1.0 cm optical pathway quartz cuvette was employed for solutions.

III. Results and Discussion

Theoretical Background. Early studies showed that the temperature dependence of the phosphorescence intensity of probes in both solvents[45] and polymers[46] was controlled by the extrinsic matrix barriers to torsion motions of the probe. Under steady-state conditions, in the absence of quenchers and oxygen (10^{-5} mmHg) and at low probe concentrations (10^{-4} mol L^{-1}), the phosphorescence quantum yield, ϕ_{Ph}, can be represented by

$$\phi_{Ph} = \phi_{ST}[k_{Ph}/(k_{Ph} + k_{nr})] \quad (1)$$

where ϕ_{ST} is the quantum yield of intersystem crossing, and the rate constants k_{Ph} and k_{nr} are associated with phosphorescence emission and all nonradiative deactivation processes (internal conversion and intersystem crossing), respectively. If any spectrum shift was observed, the temperature dependence of ϕ_{Ph} would be monitored by the phosphorescence emission intensity, I_P. Separation of the nonradiative deactivation rate constant, k_N, into temperature-independent and thermally activated components leads to the Arrhenius-like expression:

$$1/I_P - 1/I_0 = B \exp(-E_a/RT) \quad (2)$$

where I_0 is the phosphorescence intensity at a lower temperature, where it becomes temperature-independent. We are assuming this condition at 15 K, the lowest temperature employed in this work. The apparent activation energy, E_a, is associated with the nonradiative process controlled by the matrix-dependent energy barrier to motion of the probe.[45] Alternatively, and more useful, the equation is expressed in a logarithmic form:

$$\log[1/I_P - 1/I_0] = -E_a/RT + C \quad (3)$$

In the present work, the phosphorescence intensity values were obtained as the area element dimensioned 5 nm around the phosphorescence, λ_{maxPh}, or fluorescence, λ_{maxF}, maximum of every probe spectrum: Xt at 435 nm, Bp at 445 nm, F0 at 405 nm (λ_{maxF}) and 495 nm (λ_{maxPh}), F7 at 410 nm (λ_{maxF}) and 500 nm (λ_{maxPh}). The activation energy, E_a (Tables 3 and 4), was obtained from the slope of the Arrhenius plot defined by eq 3. It is important to point out that the Arrhenius plot will be linear only if a single apparent activation was involved in the entire process.

Spectral Properties of the Probes in the Polymer Films. Luminescent spectra of each probe dissolved in poly(*n*-alkyl methacrylate)s and polystyrene are showed in Figure 1. The Xt ($\lambda_{maxPh} \approx 400-404$ nm) and Bp ($\lambda_{maxPh} \approx 412-416$ nm) wavelength peaks for phosphorescence spectra (Figure 1, A and B, respectively) are within the experimental error range (Table 2). On the basis of these spectral profiles, the low-lying triplet state can be ascribed to $\pi-\pi^*$ and $n-\pi^*$ transitions for Xt and Bp, respectively. A similar trend as seen for PS was also obtained for F0 (Figure 1C) (472−469 nm) and F7 (470−473 nm) (Figure 1D) in PS and poly(*n*-alkyl methacrylate)s (Table 2).[37,48] Comparing the similarity among the phosphorescence spectra for these probes either in PS or in poly(*n*-alkyl methacrylate)s, we can assume that they are also located in low-polar environments of the polymer matrices. Moreover, compared to nonpolar solvents, the phosphorescence spectra of these molecules dissolved in the polymer matrices were always shifted to the red. Similar red shifts were reported for aromatic hydrocarbons in polyethylene, compared to aliphatic solvents, that were explained by the higher polarizability of the polymer matrix compared to the normal solvents.[48]

In addition to the phosphorescence emission, F0 and F7 dissolved in the poly(*n*-alkyl methacrylate)s exhibited an extra broad band with maximum emission at ca. 400−412 nm. These bands were observed at the wavelength range reported for the fluorescence emission of protonated molecules[37] (Table 2) (λ_{maxF} at 405 and 416 nm for F0 and F7, respectively). Although the poly(*n*-alkyl methacrylate)s are well-known basic polymers, the presence of acidic groups in our samples has also been detected by other basic dyes. As described earlier, an exhaustive extraction processes was unable to remove these groups that were attributed to some copolymerized acid groups remaining in the polymer chains.[41]

The dual fluorescence and phosphorescence emissions for F0 and F7 molecules in poly(*n*-alkyl methacrylate)s were due to the distribution in two types of polymer microenvironments. Some molecules were located in acidic sites, interacting by hydrogen bonding with the matrix and exhibiting mainly fluorescence emission. The other portion of the molecules was located in nonprotic low-polar sites, presenting the usual phosphorescence emission, similar to that in a PS matrix. The low polarity of these sites requires that the probes are surrounded by the alkyl segments of the polymer side chain. As a consequence of this heterogeneous probe distribution, every probe assembly is detecting relaxation processes of different regions of the polymer matrix. Heterogeneous dye distribution in polymer matrices has also been observed in other polymer systems where the specific dye/polymer interaction is the driving force controlling the dye distribution.[49]

Table 2. High-Energy Maximum Emission Wavelength (nm) for Phosphorescence (Ph) and Fluorescence Emissions (F), λ_{max}[a], and Triplet Energy (kJ mol^{-1}), E_T,[b] of Probes Sorbed in Polymer Films

λ_{max} (nm) (probe)	polar solvents (E_T)	nonpolar solvents (E_T)	PS	PBMA	PEMA	PMMA
λ_{maxPh} (Xt)	405[b] (310)	388[b] (310)	404	400	401	402
λ_{maxPh} (Bp)	390[b] (287)	420[b] (287)	416	415	414	412
λ_{maxPh} (F0)	469[c] (262)	465[c] (262)	472	470	471	469
λ_{maxF} (F0)	405[d] (~300)[d]			410	412	404
λ_{maxPh} (F7)	469[c] (267)[c]	465[c] (267)[c]	473	472	471	470
λ_{maxF} (F7)	416[d] (~300)[d]			412	402	398

[a] ±1 nm, at 75 K. [b] From ref 59; polar glass (EPA). [c] Nonpolar glass (3-methylpentane).[60] [d] Polar glass (EPA), nonpolar glass (cyclohexane).[45] [e] E_{S1}: pH 0.0 (T = 298 K).[37]

Table 3. Transition Temperatures[a] and Apparent Activation Energies (E_a)[b] (kJ mol^{-1}) for Probes Sorbed in PS Films

		Xt	Bp	F0	F7
γ'-relaxation	T (K)	100	108	112	112
	E_a (kJ mol^{-1})	7	4	2	3
γ-relaxation	T (K)	144	179	183	196
	E_a (kJ mol^{-1})	20	12	9	11
β-relaxation	T (K)	197	317	291	317
	E_a (kJ mol^{-1})	52	43	76	100

[a] Error ±5%. [b] Error ±10%.

Table 4. Transition Temperatures[a–c] and Apparent Activation Energies (E_a)[b,c] (kJ mol^{-1}) (in Parentheses) for Probes Sorbed in Poly(*n*-alkyl methacrylate)s

		Xt	Bp	F0	F7
T_γ (K)	PMMA	143 (9)	148 (8)	153 (5)	156 (4)
				168 (4)*	181 (3)*
	PEMA	118 (6)	122 (4)	129 (2)	139 (2)
	PBMA	102 (7)	112 (5)	111 (3)	114 (4)
T_β (K)	PMMA	213 (32)	230 (29)	230 (20)	226 (22)
				265 (12)*	263 (11)*
	PEMA	179 (25)	195 (15)	217 (12)	225 (12)
	PBMA	152 (32)	167 (21)	208 (16)	199 (15)
T_α (K)	PMMA		325 (71)	337 (68)	343 (60)
				375 (4)*	360 (3)*
	PEMA		305 (77)	294 (45)	299 (48)
	PBMA		*245* (62)	275 (62)	265 (67)

[a] Error ±5%. [b] Italic temperature value indicates complete quenched signal; the correspondent E_a values are roughly estimated; * obtained from fluorescence intensity. [c] Error ±10%.

In discussions of photochemical reactions of aromatic ketones dissolved in polymer matrices, several processes have been reported,[5,11,12,22–24,33,38,39] including hydrogen abstraction. As indicated earlier, benzophenone exhibits well-known photochemical properties in several polymer media, and the temperature dependence of the triplet state decay profiles is controlled by the polymer matrix relaxation.[11,12,38] In hydrogen-donating matrices, the hydrogen abstraction may produce a ketyl radical and probe photodegradation, while in the case of non-hydrogen-donating matrices (like PMMA) those changes of the decay profiles were ascribed to the quenching by the ester groups.[39] In the present work, photodegradation of every probe was evaluated by measuring the emission spectra at several temperatures for 4 h which was the interval spent during an entire heating cycle of samples performing sequential spectral records. During this period no significant change of the emission intensity was observed. Furthermore, no spectral changes of the absorption spectra were detected before and after every experiment. From these two types of experiments, we consider that, under our experimental conditions (low oxygen pressure, low irradiation intensity, and low probe concentration), the most significant changes of emission intensities were due to the temperature dependence of the probe photophysical properties instead of their photochemical reactions.

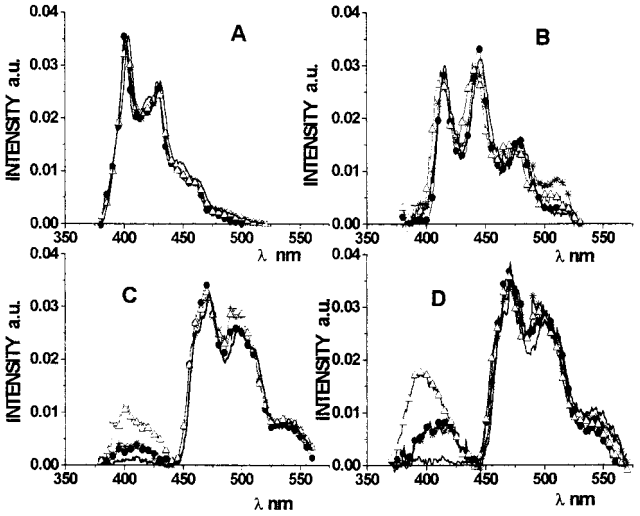

Figure 1. Phosphorescence spectra of the probes in PS (—), PMMA (△), PEMA (*), and PBMA (●). (A) Xt (λ_{exc} 340 nm), (B) Bp (λ_{exc} 340 nm), (C) F0 (λ_{exc} 320 nm), (D) F7 (λ_{exc} 320 nm). T = 75 K.

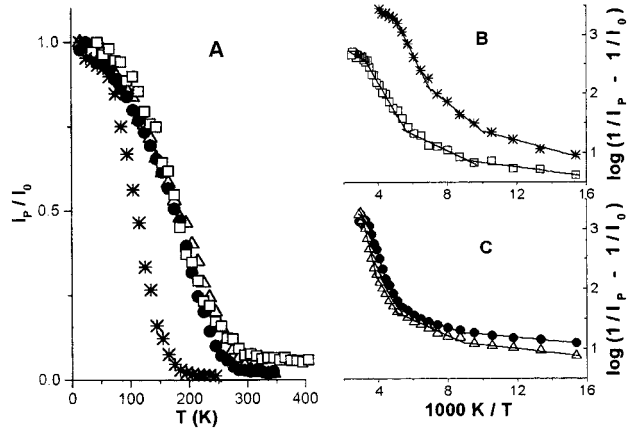

Figure 2. (A) Temperature dependence of the normalized phosphorescence intensity of probes in PS films. Arrhenius plots for $I_P \times 1/T$ for (B) Xt (*), Bp (□) and (C) F0 (●), F7 (□). I_0 was taken as 15 K.

Relaxation Processes in PS. The temperature dependence of the phosphorescence emission was initially studied for each probe in PS, as a nonpolar model medium, for which the only observed emission was the phosphorescence. The linear temperature dependence and the corresponding Arrhenius representation of the normalized I_P are shown in Figure 2. I_0 was taken at 15 K.

The probes exhibited a monotonic deactivation with the increase of temperature, but a remarkably faster process was always observed for Xt. Considering the

slope changes of the Arrhenius plots, at least three regions were observed for the temperature dependence of the phosphorescence emission. The lower temperature slope change was observed at ca. 100 K and attributed to the onset of motions of small groups containing two or three methylene or end phenyl units of polystyrene, representing the T_γ relaxation processes (Table 3).[50] It is noteworthy that the onset temperature increases with the molecular size, a typical behavior also observed for the other relaxation processes. The similarity of the E_a (ca. 3−7 kJ mol^{-1}) obtained for all probes is reflecting the sensitivity of these phosphorescent molecules to the small range motions of the polymer chain.

The next slope change occuring at 180 K was assigned to the γ-relaxation (T_γ) involving rotational motions of the phenyl rings.[5,22,38] It has been reported that the temperature dependence of ^{3}Bp* phosphorescence showed a transition at 178 K, in excellent agreement with the 179 K determined by the present work.[22,50] The reported ^{3}Bp* quenching mechanism was based on the energy-transfer process involving phenyl/carbonyl exciplex formation. An adequate orientation and short distance for both the acceptor polymer group (ester and phenyl groups) and the probe moiety (donor)[38] have defined the requirement for the mechanism. In the case of polystyrene, the necessary orientation to form the exciplex structure was only achieved when the phenyl group's rotation was allowed by the γ-relaxation process.[50] Studies of enones in glassy solvents showed that the torsional barrier of the solvent matrix controlled the temperature dependence of the phosphorescence intensity.[45]

The apparent activation energy values for the temperature dependence are also in a similar range, around 12 kJ mol^{-1} (^{3}Bp*), 9 kJ mol^{-1} (^{3}F0*), and 11 kJ mol^{-1} (^{3}F7*), except for ^{3}Xt* (20 kJ mol^{-1}), revealing a similarity among the quenching processes. Moreover, the ^{3}Xt* phosphorescence emission was almost completely quenched at $T > 197$ K, revealing a higher efficiency quenching of this molecule, in addition to its ability to detect lower onset temperatures (Table 3).

The higher temperature transition was observed around 310 K, and then every probe was completely deactivated. This temperature has been attributed to the onset of the β-relaxation process (290 K), assigned to motions of small segments of the main chain.[38,51] The calculated apparent activation energy values were distinct for each probe, revealing the different pathways for the deactivation of the triplet molecules induced by these relaxation processes (Table 3).

In addition to the exciplex formation involving the probe carbonyl group and polymer phenyl ring, several other types of quenching processes of carbonyl molecules should be considered. Among them, we must consider quenching by molecular oxygen, hydrogen abstraction reaction by the ketones configured by the n−π* transition,[38] and conformational changes of the probes induced or allowed by the polymer relaxation processes. Then, the relative importance must be evaluated, since all of these can increase the efficiency of the quenching processes, changing the slope of the Arrhenius plots.

The relative importance of the quenching by molecular oxygen was initially neglected because the samples prepared by casting were dried in a vacuum oven; the measurements were performed at low pressure (10^{-4} mmHg) under continuous pumping during both the heating and the cooling cycles. Although we did not measure the decay of the ketyl radicals eventually produced by hydrogen abstraction, we are assuming that the efficiency of this process is low due to the lower molecular decomposition under our experimental conditions.[38,52] Actually, we did not succeed in detecting any probe degradation after the experiments. Thus, we attributed these slope changes to modifications of probe photophysical properties induced by the polymer relaxation processes. It was pointed out by Horie et al.[38,39] that the rate constant for hydrogen abstraction by the benzophenone triplet from the polystyrene was very small compared with the quenching rate constant for the same molecule in solution. Following this statement, we are assuming that the lower photochemical efficiency cannot explain the temperature dependence and the discontinuity of the Arrhenius plot compared to the photophysical quenching of the triplet ketones.

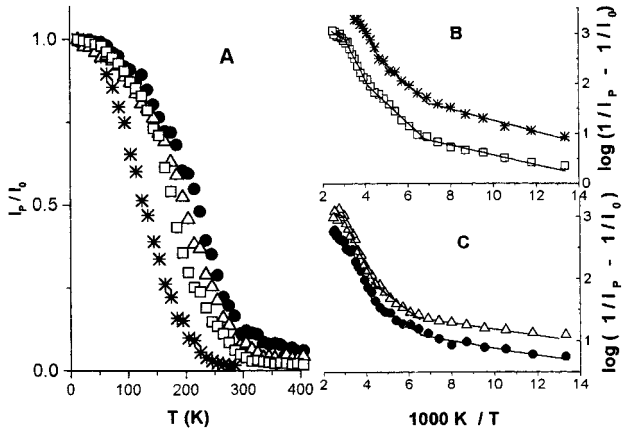

Figure 3. (A) Temperature dependence of the normalized phosphorescence intensity of probes in PMMA films. Arrhenius plots for $I_P \times 1/T$ for (B) Xt (*), Bp (□) and (C) F0 (●), F7 (□). I_0 was taken as 15 K.

In conclusion, we ascribed the higher temperature relaxation process to the free rotation of the probe phenyl moieties allowed by the free volume produced by rotation of longer macromolecular segments.

Relaxation Processes of Poly(*n*-alkyl methacrylate) Films. Following the same approach described for the photophysical behavior of the probes in PS, the linear and the Arrhenius plots represent the temperature dependence of the normalized phosphorescence intensity for each probe in poly(*n*-alkyl methacrylate) matrices (Figures 3, 5, and 6). The temperature transition (intercept) and activation energy (slope) defined for each probe are presented in Table 4. Moreover, we observed dual emissions for F0 and F7 in poly(*n*-alkyl methacrylate)s (Figure 1), and thus, we also obtained the linear and Arrhenius plots for fluorescence emission (Figure 4).

Again, the slope changes of the Arrhenius curves for the phosphorescence emission reflect modifications of the quenching process efficiencies of the excited triplet state convoluted with polymer relaxation processes. Similar to polystyrene, at least three different regions for the temperature dependence of the phosphorescence intensity of each probe (poly(*n*-alkyl methacrylate)) were detected, assigned as γ-, β-, and α'-relaxations, toward higher temperatures (Figures 3, 5, and 6) (Table 4).[5,11,12,38]

The lower temperature processes (γ-relaxation), T_γ, were attributed to rotation of the α-methyl groups bound to the main chain (Scheme 2).[22,38] Again, the onset temperature for α-methyl relaxation for PMMA in-

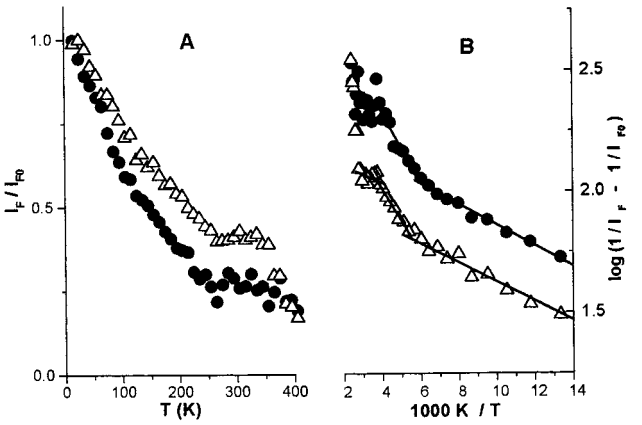

Figure 4. (A) Temperature dependence of the normalized fluorescence intensity of F0 (●) and F7 (□) in PMMA. (B) Arrhenius plots for $I_P \times 1/T$ for F0 (●) and F7 (□). I_{F0} was taken as 15 K.

Scheme 2

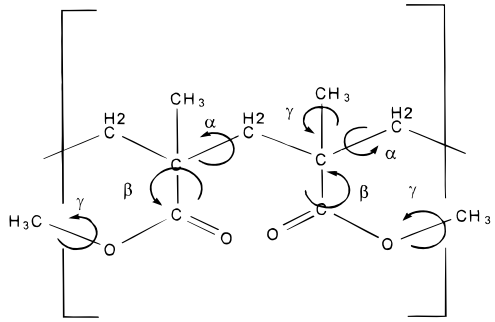

creases with the probe size, from 143 K (Xt) to 156 K (F7), in agreement with other reported values.[22] The higher onset temperatures observed for F0 and F7 were explained by the self-protection of the probe moiety produced by their phenyl substituent inhibiting the exciplex formation between the probe moiety and the polymer segment. Then, the size of the polymer *n*-alkyl segments (48−99 Å^3) involved with the relaxation process must be larger than the size of the probe substituent group (phenyl group 75 Å^3) to produce a significant modification of the probe photophysical properties. If the additional free volume will not be enough to allow the librational mode of the substituent group, the probe will be less sensitive to the polymer relaxation process.

The calculated values of the apparent activation energies for the flavone (F0 and F7) triplet state quenching produced by the α-methyl relaxation were lower than for Xt and Bp (Table 4).[22] Furthermore, both the temperature and the activation energy decrease with the increase of the alkyl side group along the methacrylate series. This general trend suggests that the larger available free volume for longer *n*-alkyl-groups ($v_w = 99$ Å^3) makes more favorable the rotations of both the α-methyl and the alkyl side groups. Assuming this as a reason for lower flavone activation energies, we considered that the phenyl moieties of these larger molecules, absent in both Bp and Xt, were responsible by an additional pathway for the quenching processes.

The next slope change, observed around 220 K for PMMA, was attributed to β-relaxation (T_β). The value for the onset temperature was also dependent on the size of the polymer *n*-alkyl side group, and again, larger molecules detected the onset at higher temperatures. The PMMA onset temperature was detected at 230 K from the slope change (Table 4), in agreement with values reported for PMMA, ca. 233 K.[38] The β-relaxation was attributed to motions of the ester moieties in poly(*n*-alkyl methacrylate)s, suggesting that the main contribution to the quenching mechanism was the energy transfer from probe moiety to the PMMA ester group.[5,11,12,38]

The triplet energy level reported for PMMA is E_T = 297−301 kJ mol^{-1};[53,54] this quenching mechanism is more efficient to ^{3}Xt*, E_T 310 kJ mol^{-1}, than ^{3}Bp*, E_T 287 kJ mol^{-1}, ^{3}F7*, E_T 267 kJ mol^{-1}, and ^{3}F0*, E_T 262 kJ mol^{-1}, roughly in the same order of the onset temperatures probed for the β-process. As emphasized by Horie et al., the quenching involving the non-single-exponential decays for benzophenone was only observed for probes with the triplet state energy lower than the polymer matrix, and the main quenching mechanism involved the energy-transfer processes from the probe to the polymer ester moieties.[55] It is worth noting that Horie et al. analyzing the system ^{3}Bp*/PMMA by triplet transient spectroscopy supported that the diffusion process below T_g was caused by rotation of the Bp and segmental motion within a few monomer units of the matrix polymer at short distance.[55]

In addition, it was recently reported that the β-process in PMMA occurred by preferential flip of the side group and that it was coupled, to some extent, with the main-chain motions (α-process) (Scheme 2).[6] The coupling mechanism between α- and β-processes in poly(*n*-alkyl methacrylate)s has been studied considering several types of experimental techniques and the relative importance of the *n*-alkyl side groups.[10,56] As an example, two simultaneously and coupled α- and β-processes were reported for PEMA at $T > T_g$, whereas only one process, a β-process, was observed below T_g.[10] ^{3}Xt* was completely quenched at $T > T_\beta$, showing a very high quenching efficiency from the oscillation of the *n*-alkyl group of the polymer chain. Furthermore, a longer *n*-alkyl group made easier both the flip motions of these segments and the coupling with the rotational motion of the main-chain motion (α-process). Consequently, T_β was expected at lower temperatures for longer *n*-alkyl methacrylate. Since we have postulated a convolution of alkyl group and probe sizes, the efficiency of the quenching process should be higher for the smaller (Xt and Bp) as opposed to the larger molecules (F0 and F7) and must be higher for longer *n*-alkyl segments.

Although the T_β temperature values determined by several techniques were similar, the apparent activation energies were 29 and 32 kJ mol^{-1} for ^{3}Bp* and ^{3}Xt*, respectively, which are completely different from those determined either by dielectric relaxation, 74 kJ mol^{-1},[10] or by multidimensional ^{13}C NMR, 72 kJ mol^{-1}.[9] Differences of activation energies determined by different techniques for the same type of relaxation process reflect differences in the kinetic description of the phenomenon and may be attributed to differences in the nature of the involved processes.[57] However, the apparent activation energies determined using luminescence techniques are very similar to the values determined in the present work for all relaxation processes.[22−25]

The higher temperature relaxation determined from the temperature dependence of the phosphorescence emission was at ca. 325−343 K. Again, larger molecules were suffering photophysical changes at higher temperatures, and longer alkyl side groups decrease the

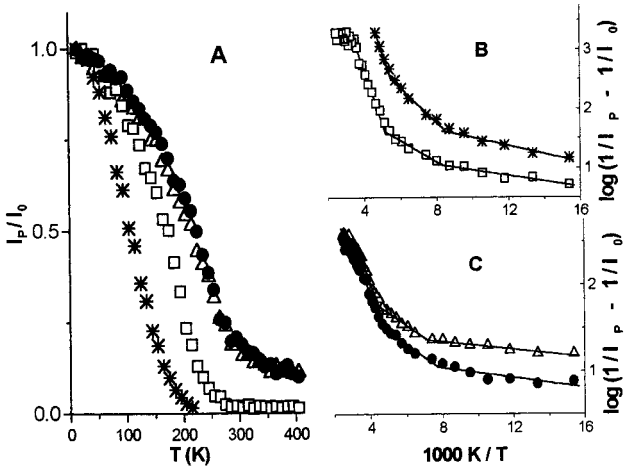

Figure 5. (A) Temperature dependence of the normalized phosphorescence intensity of probes in PEMA films. Arrhenius plots for $I_P \times 1/T$ for (B) Xt (*), Bp (□) and (C) F0 (●), F7 (□). I_0 is taken as 15 K.

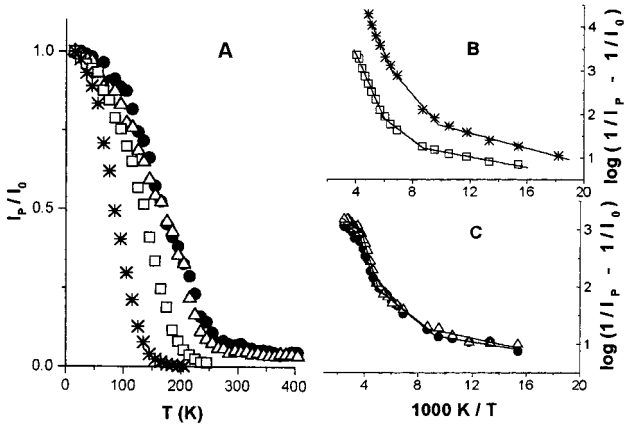

Figure 6. (A) Temperature dependence of the normalized phosphorescence intensity of probes in PBMA films. Arrhenius plots for $I_P \times 1/T$ for (B) Xt (*), Bp (□) and (C) F0 (●), F7 (□). I_{F0} was taken as 15 K.

onset temperatures. This was ascribed to α′-relaxation for poly(*n*-alkyl methacrylate)s and was interpreted as coupled main-chain and side-group motions occurring below T_g.[10] For PMMA, the onset temperatures ($T_{\alpha'}$) were 325, 337, and 345 K for ^{3}Bp*, ^{3}F0* and ^{3}F7*, respectively, far below the PMMA T_g, ca. 367 K.[11,12,22] It was also reported that the $T_{\alpha'}$ for the ^{3}Bp*/PMMA system was observed at 313 K.[53] Similarly to PMMA, the onset of the α′-relaxation process for other poly(*n*-alkyl methacrylate)s followed a sequential decrease of the temperature for longer alkyl side groups and always occurred at temperatures below the glass transition. As stressed earlier, larger probes detected higher onset temperatures that were attributed to their sensitivity to coupled motions of shorter and longer segments of the polymer chain.

We observed fluorescence emission of flavones (F0 and F7) dissolved in the poly(*n*-alkyl methacrylate)s (Figure 5) that was attributed to their protonated forms.[37] A probe distribution in the polymer matrix was assumed among the nonprotic phosphorescent and protic fluorescent sites. Following the same approach, we analyzed the temperature dependence of the fluorescence intensity and the slope changes of the linear or Arrhenius plots defining the onset temperature for relaxation processes of the polymeric fluorescent sites. Since the flavone fluorescence emissions in PEMA and PBMA were very weak, only results with PMMA are presented and discussed (Table 3). The relaxation temperatures determined using the temperature dependence for the fluorescence emission for both flavones were always higher than for phosphorescence emissions, revealing that these probes in those sites were submitted to different interactions with the polymer chains. For example, the PMMA γ-relaxations were detected at 265 and 263 K, respectively, with similar E_a of 12−11 kJ mol^{-1} (Table 4) by the fluorescence intensity of the protonated flavones ^{1}F0* and ^{1}F7*.

The phosphorescence emissions of F0 and F7 in PMMA were completely quenched at $T > 350$ K while their fluorescence emissions remained detectable at 400 K, above the PMMA glass transition temperature. Using the temperature dependence of the fluorescence emission, another transition at 360 ± 5 K was detected that was coincident with the PMMA glass transition measured by DSC. Since the fluorescence emission was occurring in protic sites, we assumed that the mechanism required long-chain motions including eventual rupture of interchain hydrogen bonds.

As reported earlier,[29,31] fluorescent molecules are more useful than phosphorescent ones to follow higher temperature polymer relaxation processes due to their shorter lifetime and different quenching mechanisms. The quenching mechanisms for shorter-lived electronic states require an acceptor energy group in the immediate vicinity of the donor moiety, either forming an exciplex during the lifetime of the singlet state or creating alternative radiative energy-transfer process pathways. Changes in the slopes of the Arrhenius plot must be related to modifications of these quenching efficiencies. Since the free volume produced by the coupled alkyl ester group and main-chain motions were large, the rotation of probe substituent groups should be completely free, being the principal pathway for complete deactivation.

IV. Conclusions

The aim of this work was the study of photophysical properties of four luminescent carbonyl molecules (xanthone, benzophenone, flavone, and 7-methoxyflavone) with different shapes and sizes, dissolved in polystyrene (nonpolar) and poly(*n*-alkyl methacrylate)s (polar) (PMMA, PEMA, and PBMA) matrices. The photophysical properties of these molecules were dependent on the probe−polymer interactions, and particularly for flavones in poly(*n*-alkyl methacrylate)s, both fluorescence and phosphorescence emissions were observed. Then, while flavones (F0 and F7) were distributed among protic and polar nonprotic sites, exhibiting fluorescence (protonated) and phosphorescence (neutral) emissions, respectively, xanthone and benzophenone have not exhibited spectral differences.

We also studied the temperature dependence of the emissions in an attempt to correlate these data to several possibilities of polymer relaxation processes. These processes modified the photophysical efficiencies, which was reflected in changes of the Arrhenius plots for the temperature dependence of the emissions. Changes of the quenching pathways relative efficiencies were explained by the convolution of several factors, including the free-volume changes produced by the polymer side group, the relationship between the molecular probe and the polymer segment sizes, and the

orientation and distance for the exciplex pair formation. Therefore, the apparent activation values were related to the convolution of all these effects.

We are assuming that the systematically lower E_a values obtained for flavones indicate a weaker coupling between probe and the shorter polymer segments, producing a less efficient quenching process. In other words, the presence of the phenyl substituent in the benzopyrone ring inhibited coupling with the ester group required to form the ring−ester exciplex necessary for the quenching process. Indeed, the less protected ^{3}Xt* and ^{3}Bp* moieties (smaller molecules) were efficiently quenched at lower temperatures, demonstrating a higher sensitivity to motions of shorter polymer segments as the onset of the polymer side-group (β-relaxation process) flip motions. Furthermore, since the flavone fluorescence and phosphorescence emissions were ascribed to molecules interacting differently with the matrices, the onset temperatures and the slope changes were assigned to different polymer relaxation processes. In conclusion, by using a probe with dual emissions sensitive to different sites such as polar nonprotic and polar protic microenvironments, we were able to detect each polymer relaxation process.

The relative importance of the polymer side-group size for relaxation processes was demonstrated by the sequential decrease of the relaxation temperatures with the increase of the *n*-alkyl-group size for PMMA, PEMA, and PBMA homopolymers. Nevertheless, the apparent activation energy involved with every relaxation processes was not following any sequential trend for an individual probe, suggesting that the precise interpretation of this parameter requires additional information about the specific probe−polymer interaction. Among the effects involved with the whole phenomenon, we should consider the convolution of the thermal-activated motion of the polymer side group (dependent on its size), the side-group/main-chain coupled motions, and the quenching efficiencies of the ester/probe exciplex formed during the probe excited state.

In conclusion, the results reported here showed that the polymer relaxation processes could effectively modify the photophysical properties of molecular probes. Despite the complexity of these processes, the results showed that the onset temperature for every relaxation processes could be determined. Taking into account that smaller molecules (Xt and Bp) were sensing the onset temperatures of shorter segments, larger probes (F0 and F7) were sequentially sensing the coupled short- and main-chain motions. These results confirmed the relevance of changing the molecular structure (shape and size) to follow polymeric motions during secondary relaxation. Additionally, they were showing that either phosphorescent or fluorescent probes may be used to follow lower temperature relaxation processes, but fluorescent one were useful for higher temperature processes.

Acknowledgment. T.D.Z.A. thanks FAPESP for financial support. M.C. acknowledges a fellowship from FAPESP. We thank Prof. Carol Collins and Prof. Y. Takahata for useful discussions.

References and Notes

(1) Adams, G.; Gibbs, J. H. *J. Chem. Phys.* **1965**, *28*, 139.
(2) Adachi, K. *Macromolecules* **1990**, *23*, 1816.
(3) Jackel, J. *Rep. Prog. Phys.* **1986**, *49*, 171.
(4) Williams, M. L.; Landel, R. F.; Ferry, J. D. *J. Am. Chem. Soc.* **1955**, *77*, 3701.
(5) Guillet, J. *Polymer Photophysics and Photochemistry*; Cambridge University Press: Cambridge, 1985.
(6) Schmidt-Rohr, K.; Kulik, A. S.; Beckham, H. W.; Ohlemacher, A.; Pawelzik, U.; Boeffel, C.; Spiess, H. W. *Macromolecules* **1994**, *27*, 4733.
(7) Ehlich, D.; Sillescu, H. *Macromolecules* **1990**, *23*, 1600.
(8) Dhinojwala, A.; Wong, G. K.; Torkelson, J. M. *Macromolecules* **1993**, *26*, 5943.
(9) Kulik, A. S.; Beckham, H. W.; Schmidt-Rohr, K.; Ohlemacher, A.; Pawelzik, U.; Boeffel, C.; Spiess, H. W. *Macromolecules* **1994**, *27*, 4746.
(10) Garwe, F.; Schonhals, A.; Lockwenz, H.; Beiner, M.; Schroter, K.; Donth, E. *Macromolecules* **1996**, *29*, 247.
(11) Tanaka, S.; Machida, S.; Yamashita, T.; Horie, K. *Macromol. Chem. Phys.* **1996**, *197*, 4095.
(12) Li, H. L.; Ujihira, Y.; Tanaka, S.; Yamashita, T.; Horie, K. *Kobunshi-Ronbunshu* **1997**, *54*, 391.
(13) Hyde, P. D.; Evert, T. E.; Cicerone, M. T.; Ediger, M. D. *J. Non-Cryst. Solids* **1991**, *131−133*, 42.
(14) Wang, H.; Jarnagin, R. C.; Samulski, E. T. *Macromolecules* **1994**, *27*, 4705.
(15) Rendell, A. K.; Ngai, K. L.; Plazek, D. J. *J. Non-Cryst. Solids* **1991**, *131−133*, 442.
(16) Jackel, J. *J. Non-Cryst. Solids* **1994**, *172−174*, 204.
(17) Hansen, M. T.; Blumich, B.; Boeffel, C.; Spiess, H. W.; Morbitzer, L.; Zembrod, A. *Macromolecules* **1992**, *25*, 5542.
(18) Hansen, M. T.; Boeffel, C.; Spiess, H. W. *Colloid Polym. Sci.* **1993**, *271*, 446.
(19) Leisen, J.; Boeffel, C.; Dong, R. Y.; Spiess, H. W. *Liq. Cryst.* **1993**, *14*, 215.
(20) Bartos, J.; Bandzuh, P.; Sausa, O.; Kristiakova, K.; Kristiak, J.; Kanaya, T.; Jenninger, W. *Macromolecules* **1997**, *30*, 6906.
(21) Wang, C. L.; Hirade, T.; Maurer, F. H. J.; Eldrup, M.; Pedersen, N. J. *J. Chem. Phys.* **1998**, *108*, 4654.
(22) Sommersall, A. C.; Dan, E.; Guillet, J. E. *Macromolecules* **1974**, *7*, 233.
(23) Tazuke, S.; Winnik, M. *Photophysical and Photochemical Tools in Polymer Science*; Winnik, M. A., Ed.; D. Riedel Pub. Company: Dordrecht, 1986; Vol. 182, p 15.
(24) Winnik, M. *Photophysical and Photochemical Tools in Polymer Science*; Winnik, M. A., Ed.; D. Riedel Pub. Company: Dordrecht, 1986; Vol. 182, p 611.
(25) Toynbee, J.; Soutar, I. Luminescence Studies of Molecular Motion in Poly(*n*-butyl)acrylate. In *Photophysics of Polymers*; Hoyle, C. E., Torkelson, J. M., Eds.; American Chemical Society: Washington, DC, 1987; Vol. 358, p 123.
(26) Atvars, T. D. Z.; Bortolato, C. A.; Brunelli, D. D.; Sabadini, E. *J. Appl. Polym. Sci., Appl. Polym. Symp.* **1991**, *49*, 167.
(27) Atvars, T. D. Z.; Sabadini, E.; Franchetti, S. M. *Eur. Polym. J.* **1993**, *29*, 1259.
(28) Song, O.-K.; Wang, C. H.; Pauley, M. A. *Macromolecules* **1997**, *30*, 6913.
(29) Talhavini, M.; Atvars, T. D. Z.; Schurr, O.; Weiss, R. G. *Polymer* **1998**, *39*, 3221.
(30) Vigil, M. R.; Bravo, J.; Atvars, T. D. Z.; Baselga, J. *Macromolecules* **1997**, *30*, 4871.
(31) Talhavini, M.; Atvars, T. D. Z.; Cui, C.; Weiss, R. G. *Polymer* **1996**, *37*, 4365.
(32) Atvars, T. D. Z.; Dorado, A. P.; Pierola, I. F. *Polym. Networks Blends* **1997**, *7*, 111.
(33) Rusakowicz, R.; Byers, G. W.; Leermakers, P. A. *J. Am. Chem. Soc.* **1971**, *93*, 3263.
(34) Scaiano, J. C. *J. Am. Chem. Soc.* **1980**, *102*, 7747.
(35) Barra, M.; Bohne, C.; Scaiano, J. C. *J. Am. Chem. Soc.* **1990**, *112*, 8075.
(36) Liao, Y.; Frank, J.; Holzwarth, J. F.; Bohne, C. *J. Chem. Soc., Chem. Commun.* **1995**, 199.
(37) Schipfer, R.; Wolfbeis, O. S.; Knierzinger, A. *J. Chem. Soc., Perkin Trans. 2* **1981**, 1443.
(38) Itagaki, H.; Horie, K.; Mita, I. *Prog. Polym. Sci.* **1990**, *15*, 361 and references cited herein.
(39) Horie, K.; Mita, I. *Chem. Phys. Lett.* **1982**, *93*, 61.
(40) Edward, J. T. *J. Chem. Educ.* **1970**, *42*, 261.
(41) Yamaki, S. B. Master Thesis, UNICAMP, 1996.
(42) Talhavini, M.; Atvars, T. D. Z. *Photochem. Photobiol.* **1998**, *114*, 65.
(43) Sabadini, E.; Atvars, T. D. Z. *Quimica Nova* **1989**, *12*, 318.
(44) Atvars, T. D. Z.; Talhavini, M. *Quim. Nova* **1995**, *18*, 298.
(45) Beavan, S. W.; Phillips, D. *Mol. Photochem.* **1977**, *8*, 311.
(46) Rutherford, H.; Soutar, I. *J. Polym. Sci., Polym. Phys.* **1980**, *18*, 1021.

(47) Christoff, M.; Toscano, V. G.; Baader, W. J. *J. Photochem. Photobiol. A: Chem.* **1996**, *101*, 11.
(48) Zimerman, O. E.; Weiss, R. G. *J. Phys. Chem.* **1998**, *102*, 5364.
(49) Dibbern-Brunelli, D.; Atvars, T. D. Z. *J. Appl. Polym. Sci.* **1995**, *55*, 889.
(50) Yano, O.; Wada, Y. *J. Polym. Sci. A* **1971**, 669.
(51) Van Krevelen, D. W. *Properties of Polymers*, 3rd ed.; Elsevier: Amsterdam, 1990.
(52) Winnik, M. A.; Li, C. K. *J. Photochem.* **1982**, *19*, 337.
(53) Graves, W. E.; Hoefeldt, R. H.; McGynn, S. P. *J. Chem. Phys.* **1972**, *56*, 1309.
(54) MacCallum, J. R. *Eur. Polym. J.* **1981**, *17*, 209.
(55) Horie, K.; Morishita, K.; Mita, I. *Macromolecules* **1984**, *17*, 1746.
(56) Schulz, M.; Donth, E. *J. Non-Cryst. Solids* **1994**, *168*, 186.
(57) Klopffer, M.-H.; Bokobza, L.; Monnerie, L. *Macromol. Symp.* **1997**, *119*, 119.

MA990008X